

# Modeling of Casting Technology of Large-Sized Ingots from Deformable Aluminum Alloys

**Aleksandr Innokentyevich Bezrukikh**

Siberian Federal University

**Vladimir Nikolaevich Baranov**

Siberian Federal University

**Igor Lazarevich Konstantinov**

Siberian Federal University

**Sergey Borisovich Sidelnikov**

Siberian Federal University

**Aleksey Aleksandrovich Iliin**

LLC "RUSAL ETC"

**Anton Viktorovich Zavizin**

Siberian Federal University

**Dmitriy Nikolaevich Bondarenko**

JSC «Scientific and Industrial Consultants»

**Boris Petrovich Kulikov**

Siberian Federal University

**Pavel Olegovich Yuryev**

Siberian Federal University

**Denis Sergeevich Voroshilov** (✉ [d.s.voroshilov@gmail.com](mailto:d.s.voroshilov@gmail.com))

Siberian Federal University School of Non-Ferrous Metals and Material Science: Sibirskij federal'nyj universitet Institut cvetnyh metallov i materialovedenia <https://orcid.org/0000-0002-1406-3665>

**Yuriy Viktorovich Baykovskiy**

Siberian Federal University

**Evgeniy Gennadyevich Partyko**

Siberian Federal University

**Yulbarskhon Nabievich Mansurov**

Tashkent State Transport University

---

## Research Article

**Keywords:** Modeling, Casting of aluminum alloys, Rolling, Mechanical properties, Scandium, Aluminum-magnesium alloys, Heat treatment.

**Posted Date:** November 17th, 2021

**DOI:** <https://doi.org/10.21203/rs.3.rs-1034479/v1>

**License:**  This work is licensed under a Creative Commons Attribution 4.0 International License.

[Read Full License](#)

---

**Version of Record:** A version of this preprint was published at The International Journal of Advanced Manufacturing Technology on February 4th, 2022. See the published version at

<https://doi.org/10.1007/s00170-022-08817-w>.

# Abstract

Industrial technology has been developed for the semi-continuous casting of large-sized ingots from deformable aluminum alloys through the use of complex modeling, including computer modeling and physical modeling. The ProCAST and ANSYS software packages equipped with the FLUENT module were used for computer modeling. The physical modeling was carried out on a laboratory semi-continuous casting unit (SCCU), which represents a tenfold reduced physical model of an industrial casting unit for the vertical semi-continuous casting of ingots from aluminum alloys. An aluminum-magnesium alloy with the addition of 0.05% (wt.) of scandium was used as the object of modeling. The results of computer modeling were tested at the SCCU, and then computer modeling was carried out for casting a large ingot. According to the modes obtained in the simulation, an ingot with a section of 1310×560 mm was cast under industrial conditions, which had a good surface quality with the absence of casting defects. In the microstructure of an industrial ingot and an ingot cast on the SCCU, there were no primary intermetallic compounds  $Al_3(Sc, Zr)$ , which makes it possible to strengthen the alloy upon annealing. To check the manufacturability during rolling, billets with a size of 40×120×170 mm were cut from these ingots, which were hot-rolled to a thickness of 5 mm, and then cold rolled to a thickness of 1 mm. The rolling results revealed good workability of the alloy, which was reflected in the high quality of the surface and the absence of cracks at the edges of the rolled stock. The mechanical properties of sheets obtained from both ingots were at the same level, which proves the reliability of casting modes for ingots obtained by complex modeling and the validity of their use for industrial conditions of the semi-continuous casting of large ingots from aluminum alloys.

## 1 Introduction

Mastering the technology of casting large-sized ingots from new deformable aluminum alloys of the Al-Mg-Sc system [1–5], obtained in industrial conditions using semi-continuous casting machines [6], requires high energy and material costs. Also, it is dangerous due to the risk of withdrawal from building the operating equipment, therefore, it is considered relevant to carry out modeling before industrial tests [7, 8]. In metallurgy, different types of modeling are used, therefore, for each case, it is important to choose the optimal type of modeling in order to obtain the most reliable results at the lowest cost. In this work, to simulate the process of semi-continuous casting of large-sized flat ingots from deformable aluminum alloys, complex modeling, including computer modeling in ESI ProCAST, ANSYS software packages were used, and physical modeling on a laboratory semi-continuous casting unit (SCCU) was applied [6, 8].

The purpose of the work was to develop an industrial technology for the semi-continuous casting of large-sized ingots from deformable aluminum alloys through complex modeling, including computer modeling, with modeling on a physical model of a casting machine for the semi-continuous casting of aluminum alloys.

To achieve this goal, the following tasks were solved in the work:

- computer simulation of the semi-continuous casting of flat aluminum alloy ingots;
- conducting experimental testing of the casting modes developed by computer modeling on the physical model of the SCCU and studying the structure of the obtained ingots;
- testing the obtained experimental modeling modes in industrial conditions for casting large-sized ingots and studying their structure;
- study of manufacturability during rolling of ingots manufactured at the SCCU and ingot cast in industrial conditions and comparison of the quality and mechanical properties of the obtained sheet semi-finished products.

## 2 Method Of Carrying Out Research

The ESI ProCAST and ANSYS software systems equipped with the FLUENT module were used to carry out the computer modeling work.

Physical modeling was carried out on a laboratory unit for the semi-continuous casting of aluminum alloys, created at the Siberian Federal University (SibFU) with the assistance of RUSAL [6]. The installation is a ten times smaller physical model of an industrial casting unit for the vertical semi-continuous casting of ingots from aluminum alloys. The automated control system of the model ensures the accuracy of adjustment and recording of the main parameters of its operation in a wide range of values, which makes it possible to obtain the structure of cast billets under cooling conditions close to industrial ones. The versatility of the equipment layout makes it possible to use the SCCU for the production of ingots from aluminum alloys by the method of semi-continuous casting into a mold with or without heat packing. The complex also provides ample opportunities for testing prototypes of technological equipment and various technical solutions in the field of foundry production. The layout of the equipment included in the SCCU is shown in Fig. 1.

The main parts of the SCCU are two induction melting furnaces 1, mixer 2, filtration unit 3, vertical casting machine 4, metal track system 5, as well as a crane, water supply, power supply, control, and control systems. In the furnaces, alloys of given chemical composition are prepared, which in the molten state are sent through a metal path to a mixer for settling, modification, and refining with argon. After the mixer, the alloy is fed through the metal track to the casting machine, in which an ingot with a rectangular section of 60×200 mm or a round section with a diameter of up to 190 mm is formed.

The operation of the SCCU is carried out by an automated process control system (APCS), the operation diagram of which is shown in Fig. 2.

An aluminum-magnesium alloy with the addition of scandium was chosen as the object of modeling, the chemical composition of which is presented in Table 1.

Table 1  
– The chemical composition of the investigated alloy [6, 8, 9]

| Mass fraction of elements, % |      |      |      |                  |       |
|------------------------------|------|------|------|------------------|-------|
| Mg                           | Fe   | Mn   | Sc   | The sum of other | Al    |
| 5.00                         | 0.17 | 0.60 | 0.05 | 0.32             | Basis |

The alloy for the physical modeling of casting was prepared in an IAT-0.16 induction furnace. The mass of the alloy for one simulation cycle was  $50 \pm 0.1$  kg, and for its preparation aluminum of the A85 brand, magnesium of the Mg90 brand, and an aluminum alloy - 2% (wt.) scandium were used. The alloy was poured from the mixer into the mold of a casting machine with a rectangular cross-section of 60×200 mm for further use of the ingot as a billet for sheet rolling. The alloy temperature was: in an induction furnace  $800 \pm 8^\circ\text{C}$ ; in the mixer  $750 \pm 5^\circ\text{C}$ , on the mold of the casting machine  $700\text{-}705^\circ\text{C}$ . The analysis of the chemical composition of the alloy was carried out on an optical emission spectrometer Hitachi Foundry master lab.

Observer A1m light microscope (Carl Zeiss) was used to study the microstructure of the alloy.

Rolling was carried out in the laboratory of the Department of Metal Forming of the Siberian Federal University [6–9]. For hot rolling, billets with a size of 40×120×170 mm were milled from the ingot and subjected to homogenization annealing in a two-stage mode: the first heating at  $350^\circ\text{C}$  and holding for 3 h, the second heating for 1 h to  $425^\circ\text{C}$  and holding for 4 h. billets were heated to  $450^\circ\text{C}$  and rolled to a thickness of 5 mm with a single reduction of 5-10% on a two-roll mill with a roll diameter of 330 mm and a barrel length of 520 mm. The total rolling reduction was 88%. Then the sheets were annealed at  $380^\circ\text{C}$  for 1 h and rolled at room temperature on a two-roll mill LS 400 AUTO manufactured by Mario Di Maio with a roll diameter of 200 mm and a barrel length of 400 mm to a thickness of 1 mm with single reductions of 2-5%. The total reduction rate was 80%. Cold-rolled sheets were annealed at  $350^\circ\text{C}$  for 3 h, and samples were cut from them for mechanical tensile tests.

The mechanical properties of hot and cold rolled semi-finished products were determined by tensile tests at room temperature on a Walter + BaiAG LFM 400 kN universal testing machine in accordance with State Standard 1497-84.

### 3 Results And Discussion

The ProCAST software package is designed for computer modeling of all casting processes and is based on the finite element method, which provides high accuracy in describing the geometry of the casting and the shape of the design model. The complex can be used to calculate most of the processes of thermal, crystallization, metallurgical and stress-strain character. The program used in the work is based on three main solvers designed to simulate the distribution of the temperature field, hydrodynamic processes, and estimate the stresses in castings [10].

The module for calculating the heat problem allows you to simulate the processes of crystallization and the formation of defects such as shrinkage cavities and macroporosity. Crystallization simulations can be performed under a variety of conditions, such as gravity casting, recharge, low pressure, or high-pressure casting.

With the help of the hydrodynamic module, it is possible to simulate the filling of a casting mold with an alloy. The calculation of hydrodynamics in ProCAST is described by the full Navier-Stokes equation and can be carried out in conjunction with the analysis of crystallization, which is especially important when adding metal to large forms when part of the melt has already begun to solidify. The calculation takes into account the stresses arising at all stages of crystallization of the alloy in the form and the likelihood of hot cracking. The hydrodynamic solver also takes into account the toughness of the alloy, depending on its temperature. Alloy toughness can also be calculated in the ProCAST thermodynamic database.

The calculation of the stress-strain state of the casting and metal tooling takes into account thermal stresses obtained during uneven cooling of various parts of the casting, as well as mechanical stresses arising from the contact interaction of the casting and the mold.

Due to the finite element method and the solver algorithm, when calculating the stress-strain state of the casting, the geometry of the computational grid changes with the restructuring and change of the coordinates of its nodes, depending on the shrinkage of the alloy and the stresses obtained, taking into account the stiffness of the form. As a result, it is possible to evaluate the shrinkage processes in the casting that are close to reality, determine the air gap between the casting and the mold, take into account its thermal resistance, and determine the mutual influence of the casting and the mold.

In the described calculation process, the problem of unsteady heat transfer and the hydrodynamic problem of metal flow in a metal path were simultaneously solved, which made it possible to take into account real heat losses when modeling casting on a physical model. Fig. 3 shows the finite element mesh of the model under the following conditions:

- casing material - Steel 3;
- the material of the metal track cartridges is refractory concrete;
- thermal insulation material - heat-insulating concrete;
- alloy material - alloy of the Al-Mg system (Table 1);
- casting temperature -  $700 \pm 5$  °C.

Figure 4 shows a model of the process of pouring metal from the ladle of an induction furnace into the receiving bowl of the SCCU and the resulting distribution of metal flow rates. The metal flow velocity  $V$  in the flow at these technological parameters was 1.5-1.7 m/s.

Figure 5 shows the model and the distribution of the velocities of the melt along the metal path when it is moved from the receiving bowl to the mixer. The melt flow rate in this area is 0.2-0.7 m/s.

Figure 6 shows the model and the distribution of the velocities of the melt during the overflow of metal from the metal track into the mixer. The melt flow rate was 0.2-1.0 m/s.

Figure 7 shows the model and the distribution of the speeds of metal movement along the metal track after its removal from the crucible of the induction furnace. The melt flow rate is 0.2-0.6 m/s.

Figure 8 shows a model of the distribution of the temperature of the metal in the metal path, which came from the crucible of the induction furnace. The temperature of the melt is in the range of 675-700°C.

Figure 9 shows a model of a longitudinal section of a mixer furnace and the temperature distribution in it after filling with liquid metal. The melt temperature is approximately 650°C, the temperature of the heaters is 700°C, and the temperature on the walls of the mixer body does not exceed 60°C.

Figure 10 shows a model of the cross-section of the metal path and the temperature distribution in it, showing that the temperature in the lining of the mixer furnace is distributed correctly, since the temperature transition is smooth and clear, and the temperature on the walls of the body of the metal path does not exceed 60°C.

To determine the modes of casting ingots at the SCCU, which could be considered as close as possible to industrial ones, a computer simulation of casting at the SCCU was carried out in the ANSYS program, equipped with the FLUENT module. At the same time, such thermal and geometric characteristics as the aspect ratio of the cast billet, the shape, and the depth of the molten metal hole were chosen as the main criteria for the similarity of experimental and industrial types of casting.

The investigated alloy belongs to the Al-Mg system, the alloys of which are not hardened by heat treatment. Recently, however, alloying with transition metals has begun to be used to strengthen these alloys. In [5, 11–37]. It was found that the greatest strengthening effect in alloys of the Al-Mg system is exerted by doping with scandium, which can be explained by the precipitation of nanosized particles of the  $\text{Al}_3\text{Sc}$  phase from the solid solution upon annealing [38–48]. These particles effectively block mobile dislocations, stabilizing the grain structure, and thus have a strong anti-recrystallization effect for all types of semi-finished products from these alloys. During casting, the rate of cooling of the melt in the range of crystallization temperatures of the aluminum-magnesium alloy affects the scandium content in the supersaturated solid solution. The higher the cooling rate, the more alloying elements, including scandium, remain in the solid solution. Considering the high cost of scandium in magnalia, this element is partially replaced by zirconium. Then the decomposition of the solid solution during subsequent heat treatment proceeds with the release of complex dispersed crystals of intermetallic phases of the  $\text{Al}_3(\text{Sc}, \text{Zr})$  type, which, like the  $\text{Al}_3\text{Sc}$  phase, improve the physical and mechanical properties of the alloy [9, 11, 20, 23, 27–30, 35, 38–40, 42, 43, 47–50]. Therefore, in order to ensure the maximum content of scandium and zirconium in a supersaturated solid solution when casting large-sized ingots from aluminum-

magnesium alloys, high crystallization rates of the melt should be used in order to exclude the formation of primary aluminides of scandium and zirconium during crystallization and cooling of the ingot [11, 20, 24, 46, 48–51].

The authors [51] have shown that one of the indicators by which the cooling rate during crystallization of aluminum alloys can be estimated is the depth of the dimple of the liquid phase of the alloy in the mold during the main casting period. In [52], it was experimentally established that when casting ingots from aluminum-magnesium alloys doped with scandium and zirconium, the maximum depth of the dimple of the liquid phase of the alloy in the mold during the main casting period must be maintained no more than the value calculated by the formula:

$$L_h = (1 \pm 0.03) \frac{NB(H - B)}{H},$$

1

where  $L_h$  – maximum depth of a hole in liquid metal, mm;  $H$  – ingot width, mm;  $B$  – ingot thickness, mm;  $N$  – an empirical coefficient, which for industrial size ingots is 0.875;  $(1 \pm 0.03)$  – confidence interval within which the experimental results fit with a reliability of 95%.

The formula is valid for alloys of the Al-Mg system, in which the scandium concentration does not exceed 0.15% (wt.)

If the condition for the depth of the hole is met, there is no primary intermetallic compounds  $Al_3(Sc, Zr)$  in the structure of the cast ingot, since all scandium and zirconium are in a supersaturated solid solution. If the depth of the molten alloy cavity in the mold is greater than the value calculated by the formula (1), then primary intermetallic compounds  $Al_3(Sc, Zr)$  appear in the ingot structure, which practically does not have a hardening effect on the alloy. As a result, the concentration of scandium in the supersaturated solid solution decreases and, as a consequence, the mechanical characteristics of the annealed deformed semi-finished products obtained during the processing of ingots.

It should be noted that the claimed parameter - the depth of the molten alloy hole in the mold - is easy to control during the casting of the ingot, for example, using the method of ultrasonic scanning or a metal probe.

The crystallization conditions of ingots obtained at the SCCU differ from industrial ingots due to different cooling rates due to a significant difference in the sizes of their cross-sections. Therefore, the modeling of the crystallization process of ingots at the SCCU was carried out in the ANSYS program, equipped with the FLUENT module according to 5 options (Table 2).



Table 2

– Simulation options for ingot casting in ANSYS software equipped with the FLUENT module

| Option | Casting temperature, °C | Casting speed, mm/s | Water consumption, m <sup>3</sup> /h | Cooling ratio at 636-705°C, °C/s | Cooling ratio at 470-705°C, °C/s | Hole depth, mm |
|--------|-------------------------|---------------------|--------------------------------------|----------------------------------|----------------------------------|----------------|
| 1      | 705                     | 85                  | 3,5                                  | 1,5                              | 3,6                              | 97             |
| 2      | 705                     | 90                  | 3,5                                  | 1,6                              | 3,8                              | 104            |
| 3      | 705                     | 100                 | 3,5                                  | 1,6                              | 3,85                             | 116            |
| 4      | 705                     | 85                  | 2,5                                  | 1,4                              | 2,85                             | 119            |
| 5      | 705                     | 120                 | 2,0                                  | 1,45                             | 3,05                             | 92             |

In Table 2 the range of 705-636°C is limited by the casting temperature and the liquidus temperature of the investigated alloy and 636-470°C is limited by the liquidus temperature and the solidus temperature. The simulation results are presented in Fig. 11-15.

The used computer program does not provide for the possibility of setting hole depth markers; therefore, this parameter in operation was determined by manual measurement. As follows from Table 2 the maximum depth of the hole ( $L_h$ ) corresponded to option No. 4. The casting parameters for this option were tested when casting on the SCCU, which gave the following results. During the crystallization of the ingot, direct measurements of the parameter  $L_h$  with a probe gave a result of  $117 \pm 3$  mm. The ingot was characterized by good surface quality and no casting defects (Fig. 16).

A large number of phases containing iron  $Al_6(Fe, Mn)$  and  $Al_{15}(Fe, Mn)_3Si_2$  were found in the microstructure of the ingot. However, inclusions of primary intermetallic compounds  $Al_3(Sc, Zr)$  were not detected (Fig. 17).

The data obtained allow making a conclusion about the correctness of the casting modes obtained by computer simulation.

The values of the parameter  $L_h$  obtained by computer and physical modeling were substituted into formula (1), the empirical coefficient  $N$  was calculated, and it was found that its value for the ingots obtained at the SCCU should be 1.95.

It should also be noted that with an increase in the casting speed, the crystallization rate of the ingot increases, which leads to an increase in the temperature on the surface of the ingot. Reducing water consumption will reduce the rate of crystallization. Analysis of computer and physical modeling showed that on an experimental ingot with a cross-section of 60×200 mm with this tooling, casting with an average crystallization rate in the range from 1.4 to 2.8°C/s will make it possible to obtain ingots with the

structure of which primary intermetallic compounds  $Al_3(Sc, Zr)$  are absent. To achieve this crystallization rate, the casting temperature should be 705°C; the casting rate should be 85 mm/s with a water flow rate of 2.5 m<sup>3</sup>/h.

Thus, we can assume that different values of the empirical coefficient  $N$  for ingots are due to the difference in cooling rates when casting large and laboratory ingots.

A computer simulation was carried out for casting an industrial large-sized ingot with a cross-section of 1310×560 mm from an alloy of chemical composition corresponding to Table 1, according to the modes indicated in Table 3. In addition, the following conditions were set for the model: metal level 60 cm, lateral distribution of metal, metal level in the mold 35 mm. The simulation result is shown in Fig. 18.

Table 3

– Modeling parameters for casting a large-sized ingot with a cross-section of 1310×560 mm in ANSYS software equipped with the FLUENT module

| Casting temperature, °C | Cooling ratio at 636-705 °C, °C/s | Cooling ratio at 470-705 °C, °C/s | Hole depth, mm |
|-------------------------|-----------------------------------|-----------------------------------|----------------|
| 705                     | 0.5                               | 1.7                               | 275            |

Determination of the depth of the model hole showed a value of 275 mm, which is in good agreement with the calculation according to formula (1) at which  $L_h = 280$  mm.

According to the modes obtained in the simulation, a large-sized ingot with a section of 1310×560 mm (Fig. 19) was obtained under industrial conditions, which had a good surface quality and was characterized by the absence of casting defects. In the casting process, the depth of the hole at the ingot was  $L_h = 276 \pm 4$  mm. In addition, studies of the microstructure of this ingot, as well as of the ingot cast on the SCCU, showed the absence of primary intermetallic compounds  $Al_3(Sc, Zr)$  in its structure, which confirms the correctness of formula (1), as well as the correctness of the casting mode developed by modeling.

To check the manufacturability during subsequent rolling, ingots with a size of 40×120×170 mm were cut from experimental and industrial ingots, which were hot rolled to a thickness of 5 mm, and then cold rolled to a thickness of 1 mm. The rolling results showed good manufacturability, both in hot and cold rolling, which was reflected in the high quality of the surface and the absence of cracks at the edges of the rolled stock [6, 9, 38–40, 49, 53, 54]. The works [38, 53–55] also present the results on the production of welded samples from the investigated alloy, confirming the manufacturability of the obtained semi-finished products. After each type of rolling, annealing and tensile tests were carried out, which gave the following results. The mechanical properties of hot-rolled sheets 5 mm thick, rolled from both ingots, after

annealing at 380°C for 1 h were at the same level:  $R_m = 340 \pm 5$  MPa,  $R_p = 215 \pm 5$  MPa,  $A = 22 \pm 2\%$ . The mechanical properties of cold-rolled alloy sheets after annealing at 350°C for 3 h were also similar and amounted to:  $R_m = 342 \pm 5$  MPa,  $R_p = 215 \pm 4$  MPa,  $A = 19 \pm 2\%$ .

## Summary

The studies carried out allowed concluding the following. The use of complex modeling of the process of semi-continuous casting of aluminum alloys, including computer modeling and physical modeling on an experimental unit of semi-continuous casting, makes it possible to develop casting modes for new alloys. At the same time, one of the important indicators that allow to control the casting process is the depth of the molten metal hole. Industrial testing of the casting modes of ingots from an alloy of the Al-Mg system with the addition of scandium, obtained by complex modeling, showed that the structure of the ingots, as well as the mechanical properties of sheet semi-finished products from the experimental and industrial large-sized ingot, practically did not differ. This proves the reliability of the modes of casting ingots obtained by complex modeling and the validity of their application for industrial conditions of semi-continuous casting of ingots from aluminum alloys.

## Declarations

### Ethical Approval

The work contains no libelous or unlawful statements, does not infringe on the rights of others, or contain material or instructions that might cause harm or injury.

### Consent to Participate

The authors consent to participate.

### Consent to Publish

The authors consent to publish.

### Authors Contributions

The authors declare that they are all participants in the work and none of them performed only administrative functions.

### Funding

The research was carried out within the framework of the state assignment of the Ministry of Science and Higher Education of the Russian Federation (scientific theme code FSRZ-2020-0011). Use of equipment of Krasnoyarsk Regional Center of Research Equipment of Federal Research Center «Krasnoyarsk Science Center SB RAS» is acknowledged.

## Competing Interests

The authors declare about the absence of competing interests.

## Availability of data and materials

The model was developed using the commercial software package ProCAST (a trademark of the ESI Group). The author completed the calculation work of ProCAST at Siberian Federal University.

## References

1. Yu.A. Gorbunov, The Role and Prospects of Rare Earth Metals in the Development of Physical-Mechanical Characteristics and Applications of Deformable Aluminum Alloys. *Journal of Siberian Federal University. Engineering & Technologies*, 2015, 8(5), 636–645 (*In Russ*). <http://journal.sfu-kras.ru/en/article/19784> Accessed 31 Oct 2021
2. Yu.A. Filatov, A.D. Plotnikov, Structure and properties of deformed semi-finished products from aluminum alloy 01570C of the Al – Mg – Sc system for the RSC “Energia” product. *Tekhnologiya legkikh splavov* [Light alloy technology], 2011, 2, 15–26 (*In Russ*).
3. A.V. Bronz, V.I. Efremov, A.D. Plotnikov, A.G. Chernyavskiy, Alloy Alloy 1570C – material for pressurized structures of advanced reusable vehicles of RSC “Energia”. *Kosmicheskaya tekhnika i tekhnologii* [Space engineering and technology], 2014, 4(7), 62–67 (*In Russ*).
4. Yashin V.V., Aryshenskiy V.Yu., Latushkin I.A., Tepterev M.S., Substantiation of a manufacturing technology of flat rolled products from Al – Mg – Sc based alloys for the aerospace industry. *Tsvetnye Metally*, 2018, 7, 75–82. DOI: 10.17580/tsm.2018.07.12
5. Filatov Yu.A., Yelagin V.I., Zakharov V.V., New Al–Mg–Sc alloys. *Materials Science and Engineering A*, 2000, 280, 97–101. [https://doi.org/10.1016/S0921-5093\(99\)00673-5](https://doi.org/10.1016/S0921-5093(99)00673-5) Accessed 31 Oct 2021
6. Konstantinov I.L., Baranov V.N., Sidelnikov S.B., Kulikov B.P., Bezrukikh A.I., Frolov V.F., Orelkina T.A., Voroshilov D.S., Yuryev P.O., Belokonova I.N., Investigation of the structure and properties of cold-rolled strips from experimental alloy 1580 with a reduced scandium content. *Int J Adv Manuf Technol*, 2020, 109(1–2), 443–450. <https://doi.org/10.1007/s00170-020-05681-4> Accessed 31 Oct 2021
7. Konstantinov I.L., Baranov V.N., Sidelnikov S.B., Arnautov A.D., Voroshilov D.S., Dovzenko N.N., Zenkin E.Y., Bezrukikh A.I., Dovzenko I.N., Yuryev P.O., Investigation of cold rolling modes of 1580 alloy by the method of computer simulation. *Int J Adv Manuf Technol*, 2021, 112(7), 1965–1972. <https://doi.org/10.1007/s00170-020-06570-6> Accessed 31 Oct 2021
8. Mann V.K., Sidelnikov S.B., Konstantinov I.L., Baranov V.N., Dovzhenko I.N., Voroshilov D.S., Lopatina E.S., Yakiviyuk O.V., Belokonova I.N., Modeling and investigation of the process of hot rolling of large-sized ingots from aluminum alloy of the AlMg system, economically alloyed by scandium. *Mater Sci Forum*, 2019, 943, 58–65. <https://doi.org/10.4028/www.scientific.net/MSF.943.58> Accessed 31 Oct 2021

9. Baranov V., Sidelnikov S., Voroshilov D., Yakiviyuk O., Konstantinov I., Sokolov R., Belokonova I., Zenkin E., Frolov V., Study of strength properties of semi-finished products from economically alloyed high-strength aluminium-scandium alloys for application in automobile transport and shipbuilding. *Open Eng*, 2018, 8(1), 69–76. <https://doi.org/10.1515/eng-2018-0005> Accessed 31 Oct 2021
10. <https://www.esi-group.com/products/casting> Accessed 31 Oct 2021
11. F. Czerwinski, Critical Assessment 36: Assessing differences between the use of cerium and scandium in aluminium alloying. *Materials Science and Technology (United Kingdom)*, 2020, 36(3), 255–263. <https://www.tandfonline.com/doi/full/10.1080/02670836.2019.1702775> Accessed 31 Oct 2021
12. Belov N.A., Naumova E.A., Bazlova T.A., Alekseeva E.V., Structure, phase composition, and strengthening of cast Al–Ca–Mg–Sc alloys. *Physics of Metals and Metallography*, 2016, 117(2), 188–194. <https://doi.org/10.1134/S0031918X16020046> Accessed 31 Oct 2021
13. S. Mondol, T. Alamb, R. Banerjee, S. Kumar, K. Chattopadhyay, Development of a high temperature high strength Al alloy by addition of small amounts of Sc and Mg to 2219 alloy. *Materials Science & Engineering*, 2017, A687, 221–231. <https://doi.org/10.1016/j.msea.2017.01.037> Accessed 31 Oct 2021
14. Zakharov V.V., Prospects of Creation of Aluminum Alloys Sparingly Alloyed with Scandium. *Metal Science and Heat Treatment*, 2018, 60(3-4), 172–176. <https://doi.org/10.1007/s11041-018-0256-8> Accessed 31 Oct 2021
15. Zakharov V.V., Kinetics of Decomposition of the Solid Solution of Scandium in Aluminum in Binary Al – Sc Alloys. *Metal Science and Heat Treatment*, 2015, 57(7-8), 410–414. <https://doi.org/10.1007/s11041-015-9897-z> Accessed 31 Oct 2021
16. Zakharov, V.V., Rostova, T.D., Hardening of aluminum alloys due to scandium alloying. *Metal Science and Heat Treatment*, 2014, 55(11-12), 660–664. <https://doi.org/10.1007/s11041-014-9686-0> Accessed 31 Oct 2021
17. Zakharov V.V., Fisenko I.A., Some Principles of Alloying of Aluminum Alloys with Scandium and Zirconium in Ingot Production of Deformed Semiproducts. *Metal Science and Heat Treatment*, 2019, 61(3-4), 217–221. <https://link.springer.com/article/10.1007%2Fs11041-019-00403-4> Accessed 31 Oct 2021
18. Zakharov V.V., Combined Alloying of Aluminum Alloys with Scandium and Zirconium. *Metal Science and Heat Treatment*, 2014, 56(5-6), 281–286. <https://doi.org/10.1007/s11041-014-9746-5> Accessed 31 Oct 2021
19. Sun Y., Pan Q., Luo Y., Liu S., Wang W., Ye J., Shi Y., Huang Z., Xiang S., Liu Y., The effects of scandium heterogeneous distribution on the precipitation behavior of Al<sub>3</sub>(Sc, Zr) in aluminum alloys. *Materials Characterization*, 2021, 174, 110971. <https://doi.org/10.1016/j.matchar.2021.110971> Accessed 31 Oct 2021
20. Chunchang Shi, Liang Zhang, Guohua Wu, Xiaolong Zhang, Antao Chen, Jiashen Tao, Effects of Sc addition on the microstructure and mechanical properties of cast Al-3Li-1.5Cu-0.15Zr alloy. *Materials*

- Science & Engineering, 2017, A680, 232–238. <https://doi.org/10.1016/j.msea.2016.10.063>  
Accessed 31 Oct 2021
21. Yu. Buranova, V. Kulitskiy, M. Peterlechner, A. Mogucheva, R. Kaibyshev, S.V. Divinski, G. Wilde, Al<sub>3</sub>(Sc,Zr)-based precipitates in Al–Mg alloy: Effect of severe deformation. *Acta Materialia*, 2017, 124, 210–224. <https://doi.org/10.1016/j.actamat.2016.10.064> Accessed 31 Oct 2021
22. Pedro Henrique R. Pereira, Ying Chun Wang, Yi Huang, Terence G. Langdon, Influence of grain size on the flow properties of an Al-Mg-Sc alloy over seven orders of magnitude of strain rate. *Materials Science & Engineering*, 2017, A685, 367–376.  
DOI: <https://doi.org/10.1016/j.msea.2017.01.020> Accessed 31 Oct 2021
23. V. Rajinikanth, Vikas Jindal, V.G. Akkimardi, Mainak Ghosha, K. Venkateswarlu, Transmission electron microscopy studies on the effect of strain on Al and Al–1% Sc alloy. *Scripta Materialia*, 2007, 57, 425–428. DOI: <https://doi.org/10.1016/j.scriptamat.2007.04.038> Accessed 31 Oct 2021
24. K.Yan, Z.W.Chen, Y.N.Zhao, C.C.Ren, W.J.Lu, A.W.Aldeen, Morphological characteristics of Al<sub>3</sub>Sc particles and crystallographic orientation relationships of Al<sub>3</sub>Sc/Al interface in cast Al-Sc alloy. *Journal of Alloys and Compounds*, 2021, 861, 158491.  
DOI: <https://doi.org/10.1016/j.jallcom.2020.158491> Accessed 31 Oct 2021
25. Zhao Y., Zhang W., Koe B., Du W., Wang M., Wang W., Boller E., Rack A., Sun Z., Shu D., Sun B., Mi J., Multiscale characterization of the nucleation and 3D structure of Al<sub>3</sub>Sc phases using electron microscopy and synchrotron X-ray tomography. *Materials Characterization*, 2020, 164, 110353. <https://doi.org/10.1016/j.matchar.2020.110353> Accessed 31 Oct 2021
26. Jiang J., Jiang F., Zhang M., Tang Z., Tong M., Recrystallization behavior of Al-Mg-Mn-Sc-Zr alloy based on two different deformation ways. *Materials Letters*, 2020, 265, 127455. <https://doi.org/10.1016/j.matlet.2020.127455> Accessed 31 Oct 2021
27. Yuhong Luo, Qinglin Pan, Yuqiao Sun, Shuhui Liu, Yuanwei Sun, Liang Long, Xinyu Li, Xiaoping Wang, Mengjia Li, Hardening behavior of Al-0.25Sc and Al-0.25Sc-0.12Zr alloys during isothermal annealing. *Journal of Alloys and Compounds*, 2020, 818, 152922. <https://doi.org/10.1016/j.jallcom.2019.152922> Accessed 31 Oct 2021
28. Weigui Zhang, Yanmiao Wu, Hongyu Lu, Guanqing Lao, Ke Wang, Yicong Ye, Peijie Li, Discontinuous Precipitation of Nano-Al<sub>3</sub>Sc Particles in Al-Sc Alloy and Its Effect on Mechanical Property. *International Journal of Nanoscience*, 2020, 19(1), 1850047. <https://doi.org/10.1142/S0219581X18500473> Accessed 31 Oct 2021
29. Dong Q., Howells A., Lloyd D.J., Gallerneault M., Fallah V., Effect of solidification cooling rate on kinetics of continuous/discontinuous Al<sub>3</sub>(Sc,Zr) precipitation and the subsequent age-hardening response in cold-rolled AlMgSc(Zr) sheets. *Materials Science and Engineering A*, 2020, 772, 138693. <https://doi.org/10.1016/j.msea.2019.138693> Accessed 31 Oct 2021
30. Zakharov V.V., Filatov Y.A., Fisenko I.A., Scandium Alloying of Aluminum Alloys. *Metal Science and Heat Treatment*, 2020, 62, 518–523. <https://doi.org/10.1007/s11041-020-00595-0> Accessed 31 Oct 2021

31. J. Røyset, N. Ryum, Scandium in aluminium alloys. *International Materials Reviews*, 2005 50(1), 19–44. DOI: <https://doi.org/10.1179/174328005X14311> Accessed 31 Oct 2021
32. C.B. Fuller, J.L. Murray, D.N. Seidman, Temporal evolution of the nanostructure of Al(Sc, Zr) alloys: Part I – Chemical compositions of Al<sub>3</sub>(Sc<sub>1-x</sub>Zr<sub>x</sub>) precipitates. *Acta Materialia*, 2005, 53, 5401–5413. <https://doi.org/10.1016/j.actamat.2005.08.016> Accessed 31 Oct 2021
33. C.B. Fuller, D.N. Seidman, Temporal evolution of the nanostructure of Al(Sc,Zr) alloys: Part II-coarsening of Al<sub>3</sub>(Sc<sub>1-x</sub>Zr<sub>x</sub>) precipitates. *Acta Materialia*, 2005, 53, 5415–5428. <https://doi.org/10.1016/j.actamat.2005.08.015> Accessed 31 Oct 2021
34. W. Lefebvre, F. Da-noixa, H. Hallem, B. Forbord, A. Bostel, K. Marthinsen, Precipitation kinetic of Al<sub>3</sub>(Sc, Zr) dispersoids in aluminium. *Journal of Alloys and Compounds*, 2009, 470, 107–110. <https://doi.org/10.1016/j.jallcom.2008.02.043> Accessed 31 Oct 2021
35. G. Li, N. Zhao, T. Liu, J. Li, C. He, C. Shi, E. Liu, J. Sha, Effect of Sc/Zr ratio on the microstructure and mechanical properties of new type of Al–Zn–Mg–Sc–Zr alloys. *Materials Science & Engineering A*, 2014, 617, 219–227. <https://doi.org/10.1016/j.msea.2014.08.041> Accessed 31 Oct 2021
36. H. Pouraliakbar, M. Pakbaz, S. Firooz, M. R. Jandaghi, G. Khalaj, Study on the dynamic and static softening phenomena in Al–6Mg alloy during two-stage deformation through interrupted hot compression test. *Measurement*, 2016, 77, 50–53. <https://doi.org/10.1016/j.measurement.2015.08.033> Accessed 31 Oct 2021
37. M. Reza Jandaghi, H. Pouraliakbar, A. Saboori, Effect of second-phase particles evolution and lattice transformations while ultrafine graining and annealing on the corrosion resistance and electrical conductivity of Al–Mn–Si alloy. *Material Research Express*. 2019, 6(10), 1065D9. <https://doi.org/10.1088/2053-1591/ab37d5> Accessed 31 Oct 2021
38. Baranov V.N., Sidelnikov S.B., Zenkin E.Yu., Konstantinov I.L., Lopatina E.S., Yakiviyuk O.V., Voroshilov D.S., Belokonova I.N., Frolov V.A. Study on the influence of heat treatment modes on mechanical and corrosion properties of rolled sheet products from a new aluminum alloy, economically alloyed with scandium. *Vestnik of Nosov Magnitogorsk State Technical University*, 2019, 17(1), 76–81. DOI: <https://doi.org/10.18503/1995-2732-2019-17-1-76-81> Accessed 31 Oct 2021
39. Baranov V.N., Sidelnikov S.B., Bezrukikh A.I., Zenkin E.Yu., Research of rolling regimes and mechanical properties of cold-rolled, annealed and welded semi-finished products from experimental alloys of Al – Mg system, economically alloyed by scandium. *Tsvetnye Metally*, 2017, 9, 91–96. DOI: 10.17580/tsm.2017.09.13
40. I.L. Konstantinov, V.N. Baranov, S.B. Sidelnikov, E.Yu. Zenkin, P.O. Yuryev, I.N. Belokonova, Influence of Rolling and Annealing Modes on Properties of Sheet Semifinished Products Made of Wrought Aluminum Alloy 1580. *Russian Journal of Non-Ferrous Metals*, 2020, 61, 641–645. <https://doi.org/10.3103/S1067821220060115> Accessed 31 Oct 2021
41. Koryagin Yu.D., Il'in S.I., Recrystallization features of deformable aluminium-magnesium alloys with scandium. *Bulletin of the South Ural State University. Series “Metallurgy”*, 2017, 17, 1, 65–72 (*In Russ*). [https://www.elibrary.ru/download/elibrary\\_28766384\\_36767861.pdf](https://www.elibrary.ru/download/elibrary_28766384_36767861.pdf) Accessed 31 Oct 2021

42. Keith E. Knipling, David N. Seidman, David C. Dunand, Ambient- and high-temperature mechanical properties of isochronally aged Al–0.06Sc, Al–0.06Zr and Al–0.06Sc–0.06Zr (at.%) alloys. *Acta Materialia*, 2011, 59, 943–954. <https://doi.org/10.1016/j.actamat.2010.10.017> Accessed 31 Oct 2021
43. Xie J., Chen X.P., Mei L., Huang G.J., Liu Q., Investigation of the hardening behavior during recrystallization annealing in Al-Mg-Sc alloy. *Journal of Alloys and Compounds*, 2021, 859, 157807. <https://doi.org/10.1016/j.jallcom.2020.157807> Accessed 31 Oct 2021
44. Jiang J., Jiang F., Zhang M., Tang Z., Tong M., Effect of continuity of annealing time on the recrystallization behavior of Al-Mg-Mn-Sc-Zr alloy. *Materials Letters*, 2020, 275, 128208. <https://doi.org/10.1016/j.matlet.2020.128208> Accessed 31 Oct 2021
45. Jiang J., Jiang F., Zhang M., Tang Z., Tong M., Al<sub>3</sub>(Sc, Zr) precipitation in deformed Al-Mg-Mn-Sc-Zr alloy: Effect of annealing temperature and dislocation density. *Journal of Alloys and Compounds*, 2020, 831, 154856. <https://doi.org/10.1016/j.jallcom.2020.154856> Accessed 31 Oct 2021
46. M. Vlach, I. Stulíková, B. Smola, N. Zaludová, J. Cerná, Phase transformations in isochronally annealed mould-cast and cold-rolled Al–Sc–Zr-based alloy. *Journal of Alloys and Compounds*, 2010, 149, 243–248. <https://doi.org/10.1016/j.jallcom.2009.11.126> Accessed 31 Oct 2021
47. Yuhong Luo, Qinglin Pan, Yuqiao Sun, Shuhui Liu, Yuanwei Sun, Liang Long, Xinyu Li, Xiaoping Wang, Mengjia Li, Hardening behavior of Al-0.25Sc and Al-0.25Sc-0.12Zr alloys during isothermal annealing. *Journal of Alloys and Compounds*, 2020, 818, 152922. <https://doi.org/10.1016/j.jallcom.2019.152922> Accessed 31 Oct 2021
48. Dong Q., Howells A., Lloyd D.J., Gallerneault M., Fallah V., Effect of solidification cooling rate on kinetics of continuous/discontinuous Al<sub>3</sub>(Sc,Zr) precipitation and the subsequent age-hardening response in cold-rolled AlMgSc(Zr) sheets. *Materials Science and Engineering A*, 2020, 772, 138693. <https://doi.org/10.1016/j.msea.2019.138693> Accessed 31 Oct 2021
49. Yuryev P.O., Baranov V.N., Orelkina T.A. Bezrukikh A.I., Voroshilov D.S., Murashkin M.Yu., Partyko E.G., Konstantinov I.L., Yanov V.V., Stepanenko N.A., Investigation the structure in cast and deformed states of aluminum alloy, economically alloyed with scandium and zirconium. *Int J Adv Manuf Technol*, 2021, 115, 263–274. <https://doi.org/10.1007/s00170-021-07206-z> Accessed 31 Oct 2021
50. Dovzhenko N.N., Rushchits S.V., Dovzhenko I.N., Sidelnikov S.B., Voroshilov D.S., Demchenko A.I., Baranov V.N., Bezrukikh A.I., Yuryev P.O., Deformation behavior during hot processing of the alloy of the Al-Mg system economically doped with scandium. *Int J Adv Manuf Technol*, 2021, 115, 2571–2579. <https://doi.org/10.1007/s00170-021-07338-2> Accessed 31 Oct 2021
51. Napalkov V.I., Baranov V.N., Frolov V.F., Bezrukikh A.I., Melting and casting of aluminum alloys: monography. SibFU, Krasnoyarsk, 2020. <https://bik.sfu-kras.ru/shop/publication?id=BOOK1-669.7/%D0%9F%20370-028821> Accessed 31 Oct 2021
52. Kulikov B.P., Baranov V.N., Bezrukikh A.I., Zenkin E.Yu., Yuryev P.O., Stepanenko N.A., Pat. 2723578 Russian Federation. Способ полунепрерывного литья плоских крупногабаритных слитков из алюминиево-магниевого сплава, легированного скандием и цирконием. Publ. 16



Jun 2020, Bul. № 17. (*In Russ*) [https://www.fips.ru/registers-doc-view/fips\\_servlet?DB=RUPAT&DocNumber=2723578&TypeFile=html](https://www.fips.ru/registers-doc-view/fips_servlet?DB=RUPAT&DocNumber=2723578&TypeFile=html) Accessed 31 Oct 2021

53. Baranov V.N., Sidelnikov S.B., Zenkin E.Yu., Bezrukikh A.I., Konstantinov I.L., Sokolov R.E., Voroshilov D.S., Belokonova I.N., Yakivyyuk O.V. Study of the mechanical properties of semi-finished products from aluminum-scandium alloy. Bulletin of the Tula State University, 2017, 11(1), 147–153 (*In Russ*). [https://www.elibrary.ru/download/elibrary\\_30684027\\_37341897.pdf](https://www.elibrary.ru/download/elibrary_30684027_37341897.pdf) Accessed 31 Oct 2021
54. Baranov VN, Sidelnikov SB, Frolov VF, Zenkin EYu, Orelkina TA, Konstantinov IL, Voroshilov DS, Yakivyyuk OV, Belokonova IN (2018) Investigation of mechanical properties of cold-rolled, annealed and welded semi-finished products from the test alloys of Al-Mg system, economically alloyed with scandium. IOP Conf Ser: Mater Sci Eng 411: 012015. <https://doi.org/10.1088/1757-899X/411/1/012015> Accessed 31 Oct 2021
55. Dovzhenko N.N., Demchenko A.I., Bezrukikh A.A., Dovzhenko I.N., Baranov V.N., Orelkina T.A., Dementeva I.S., Voroshilov D.S., Gaevskiy V.N., Lopatina E.S., Mechanical properties and microstructure of multi-pass butt weld of plates made of Al-Mg-Zr alloy sparingly doped with scandium. The International Journal of Advanced Manufacturing Technology, 2021, 113, 785–805. <https://doi.org/10.1007/s00170-021-06665-8> Accessed 31 Oct 2021

## Figures

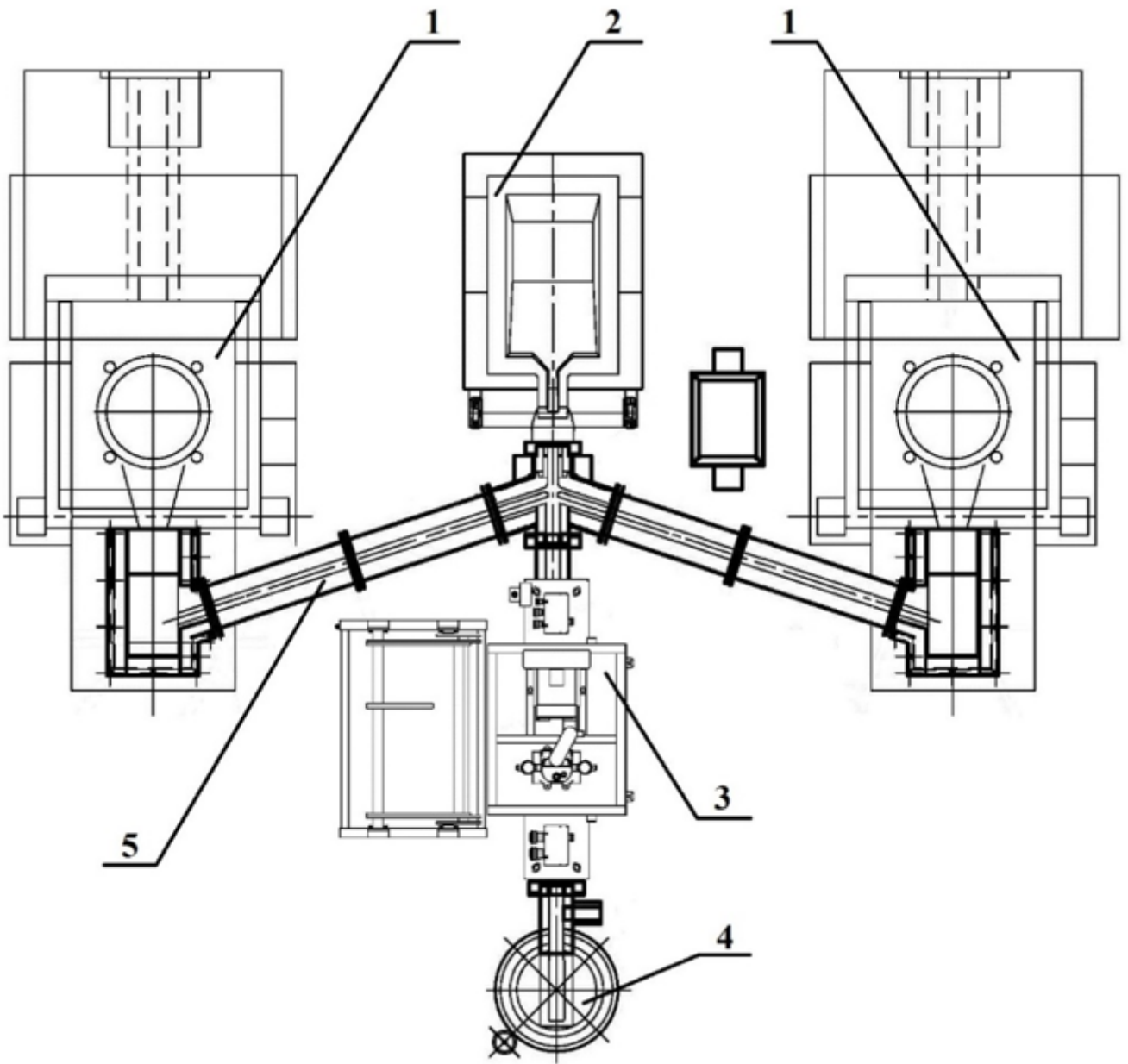


**Figure 1**

Layout of the SCCU equipment [6]: 1 – furnaces; 2 – mixer; 3 – filtration unit; 4 – vertical casting machine; 5 – metal track

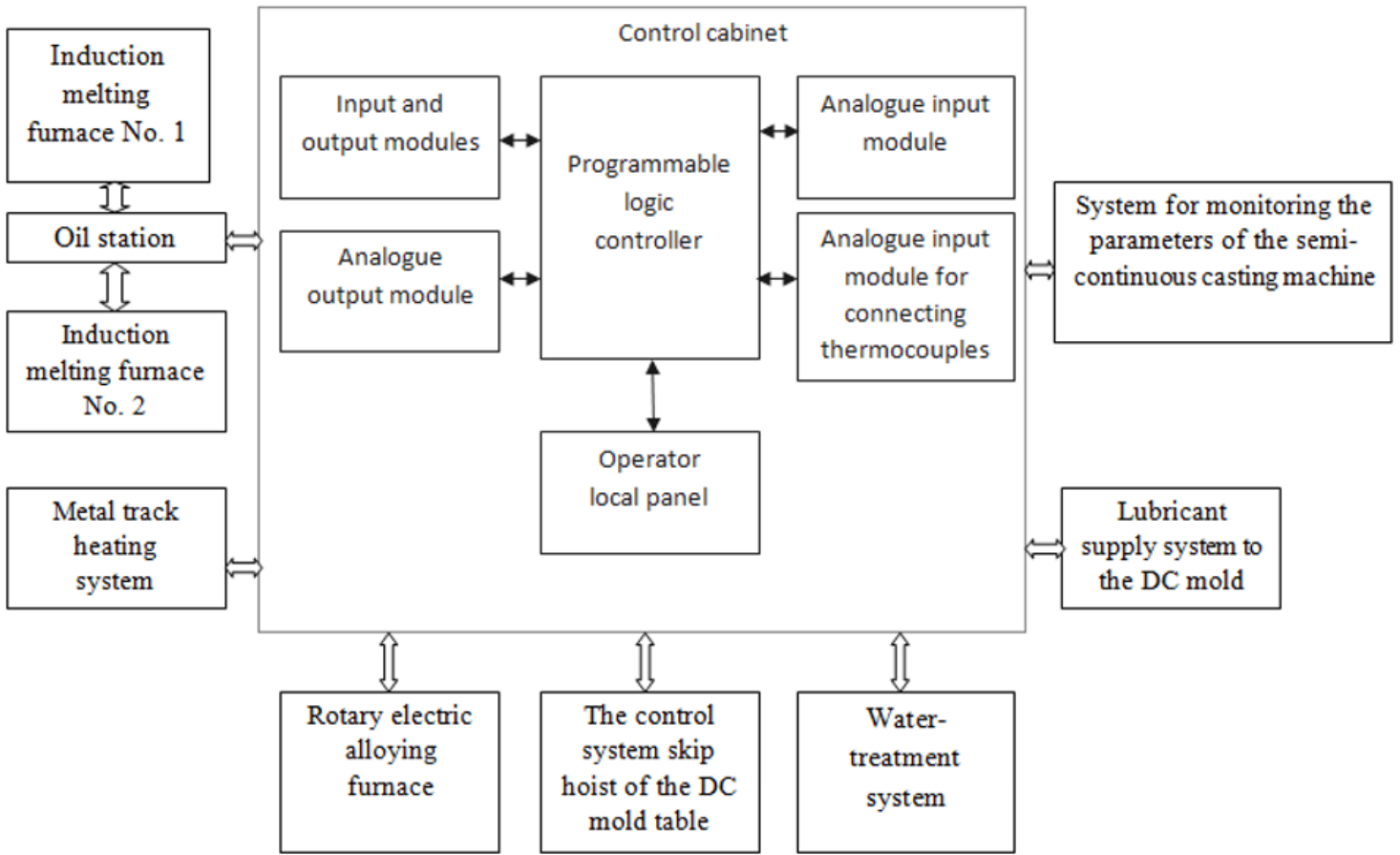


**Figure 2**

Automation system schematic of SCCU

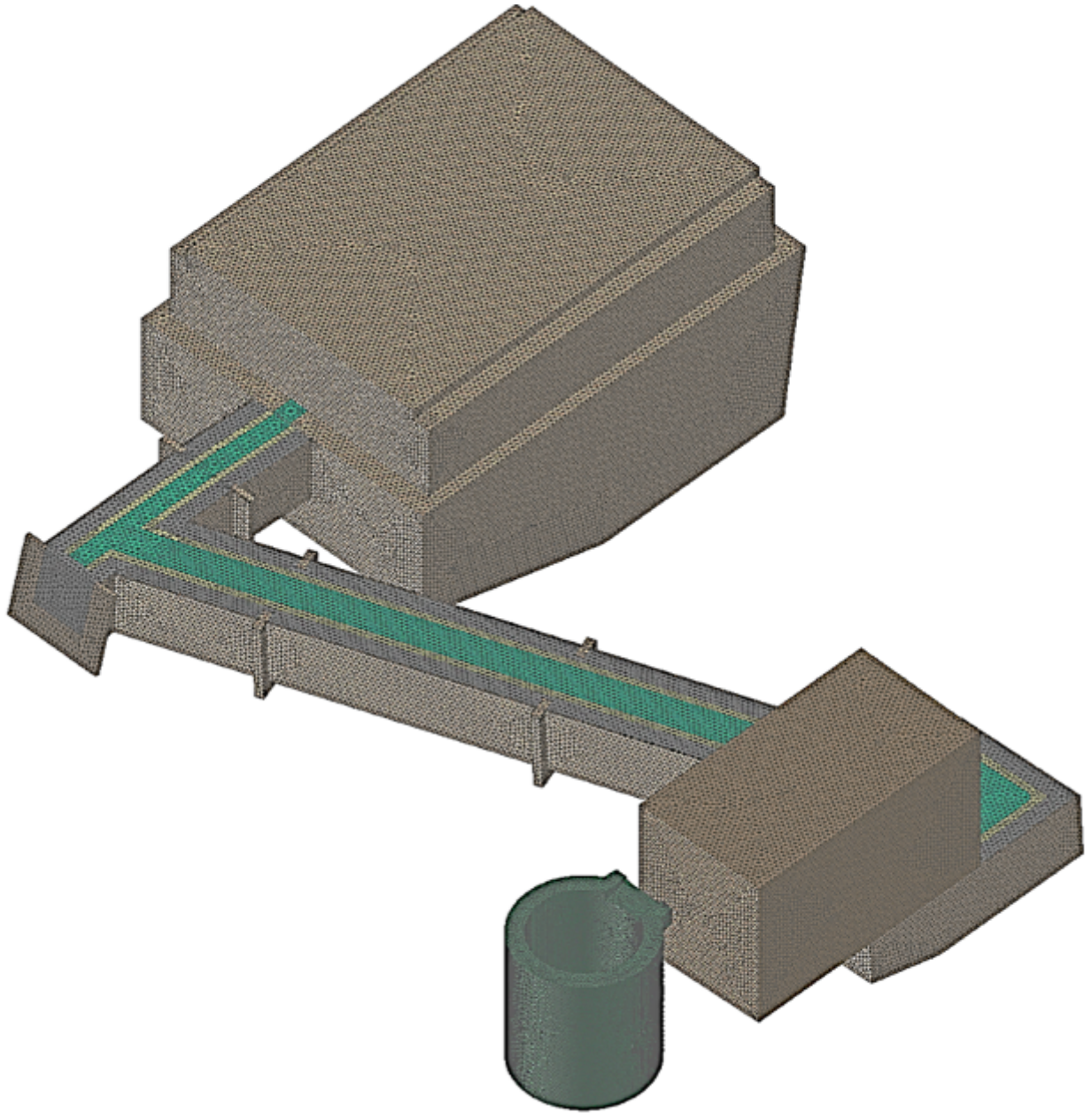


**Figure 3**

Finite element mesh of the model in the ProCAST program for calculating the overflow of melt from an induction furnace to a mixer furnace

$V, m/s$

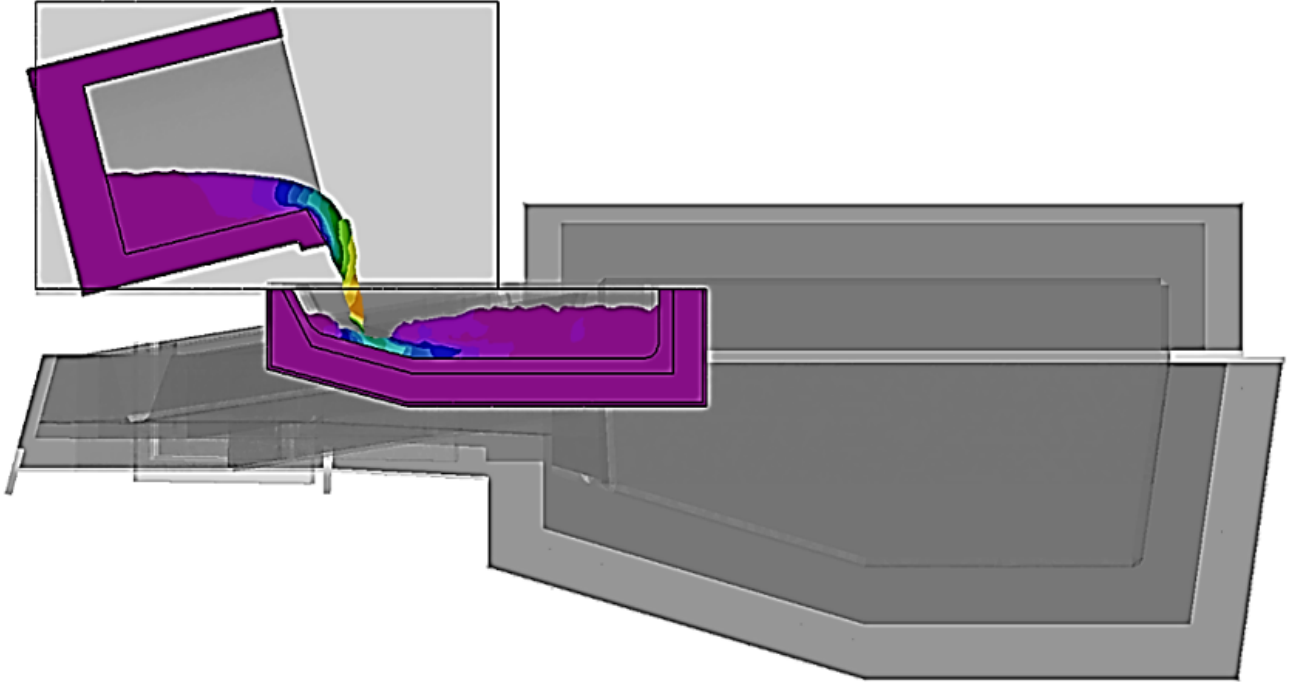
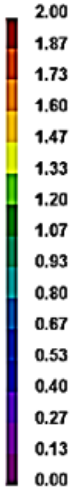


Figure 4

Model of the distribution of metal flow velocities during overflow from the ladle to the receiving bowl

$V, m/s$

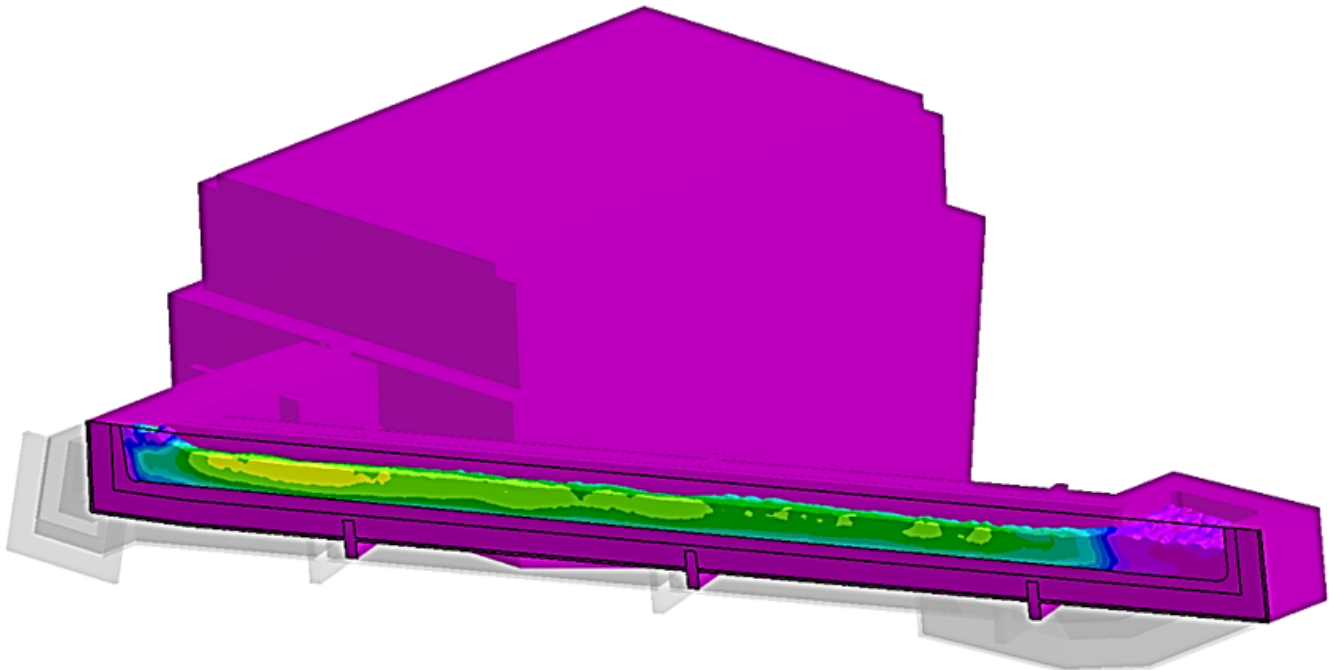
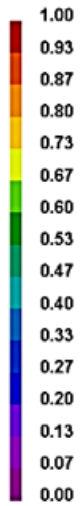


Figure 5

Model of the distribution of metal flow velocities along the trays of the metal track

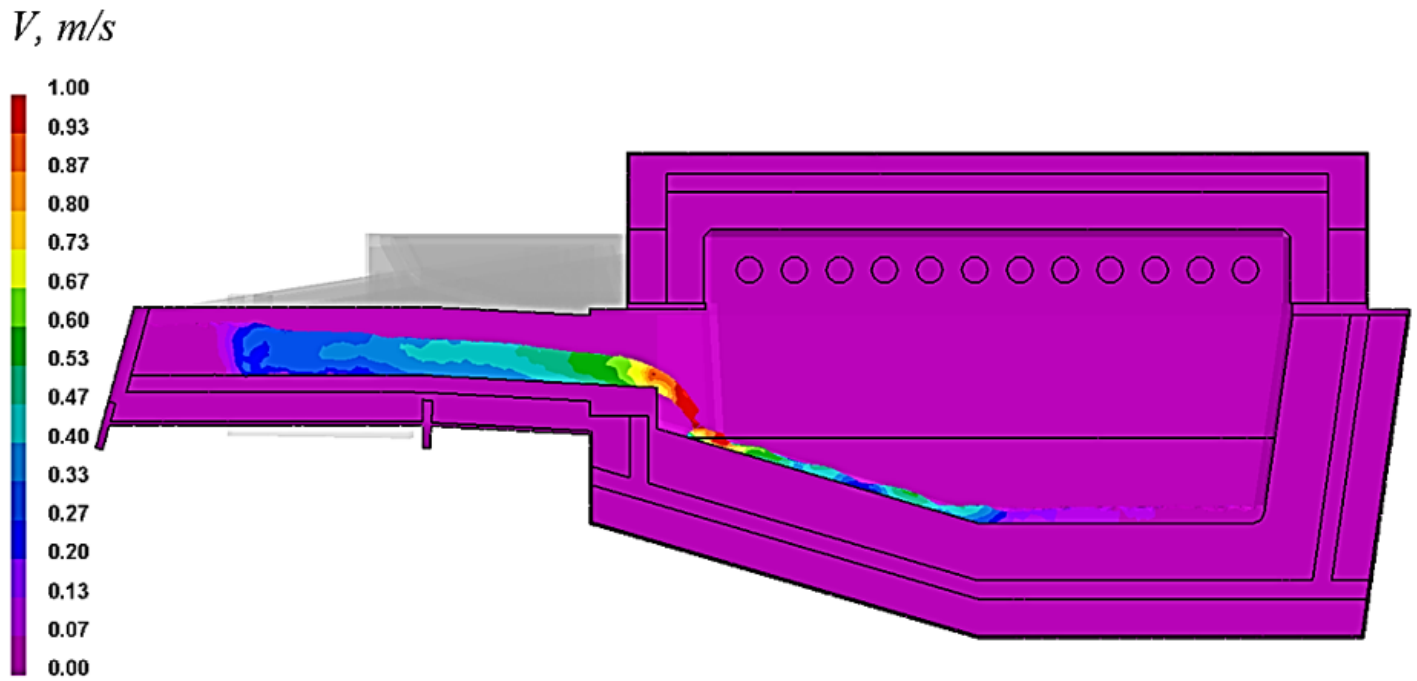


Figure 6

Model of the distribution of metal flow rates during melt pouring from metal track trays into a mixer furnace

$V, m/s$

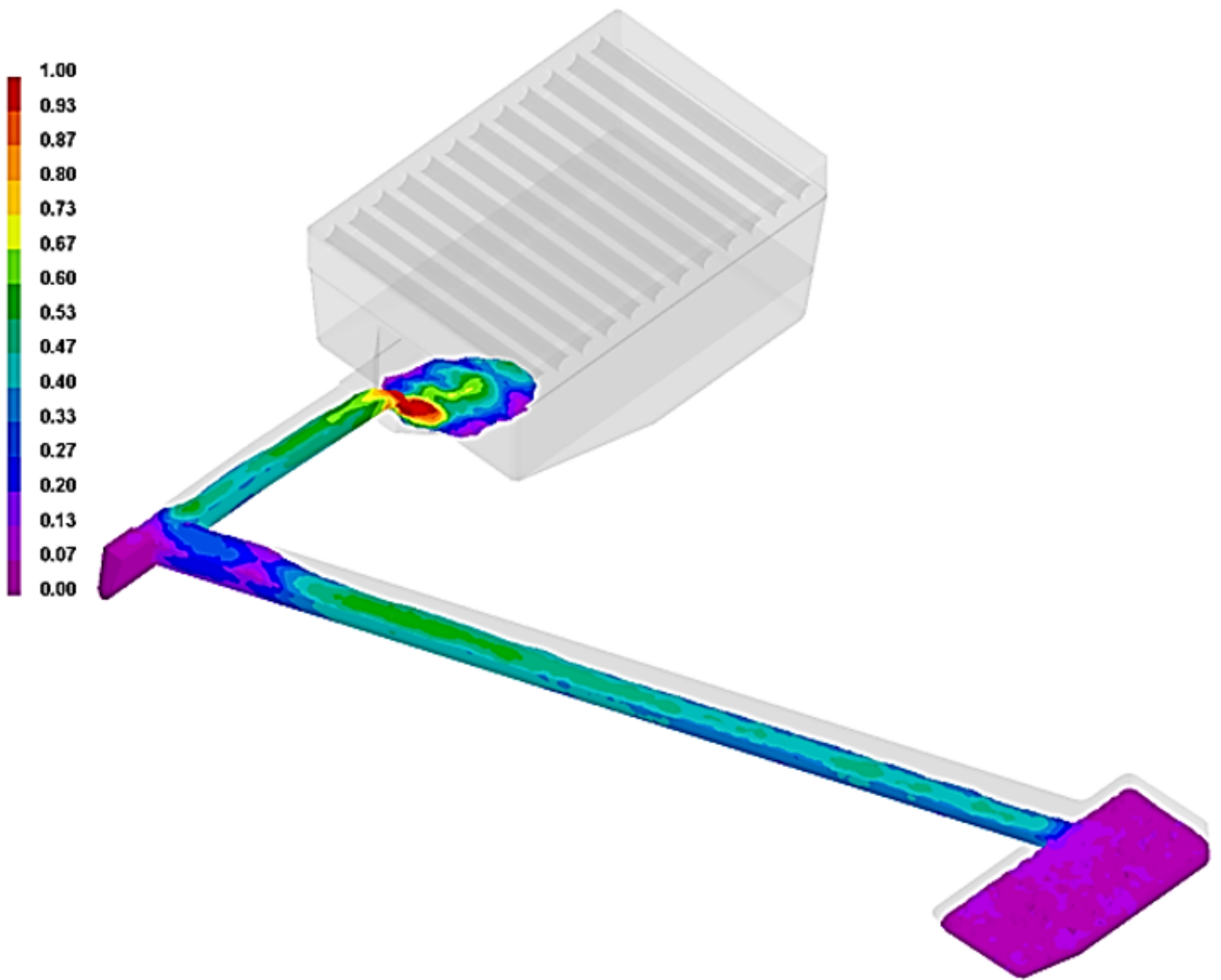


Figure 7

Model of distribution of metal flow rates during melt overflow from metal track trays into a mixer

T, °C

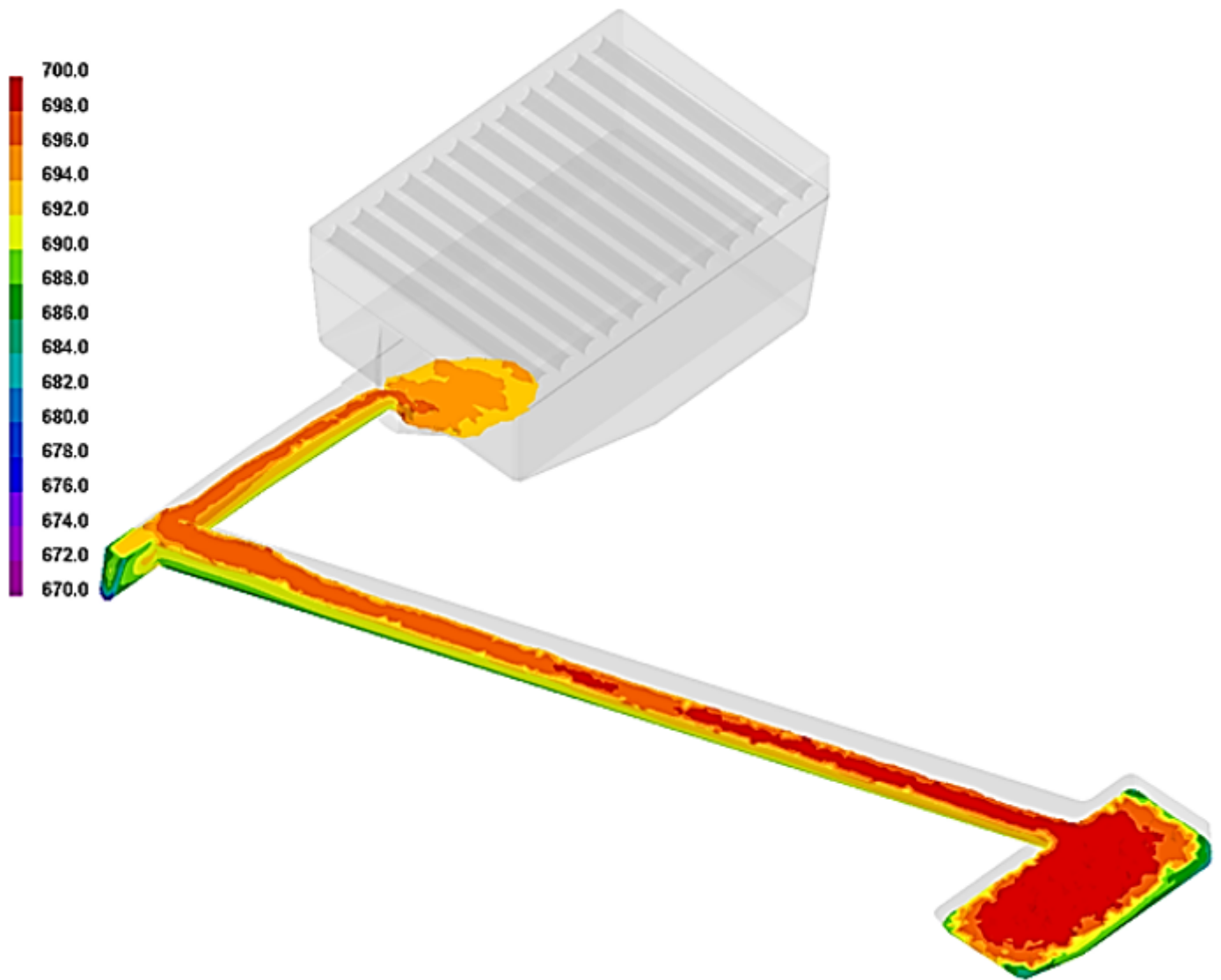


Figure 8

Model of the temperature distribution of the metal in the trays of the metal track received from the crucible of the induction furnace



T °C

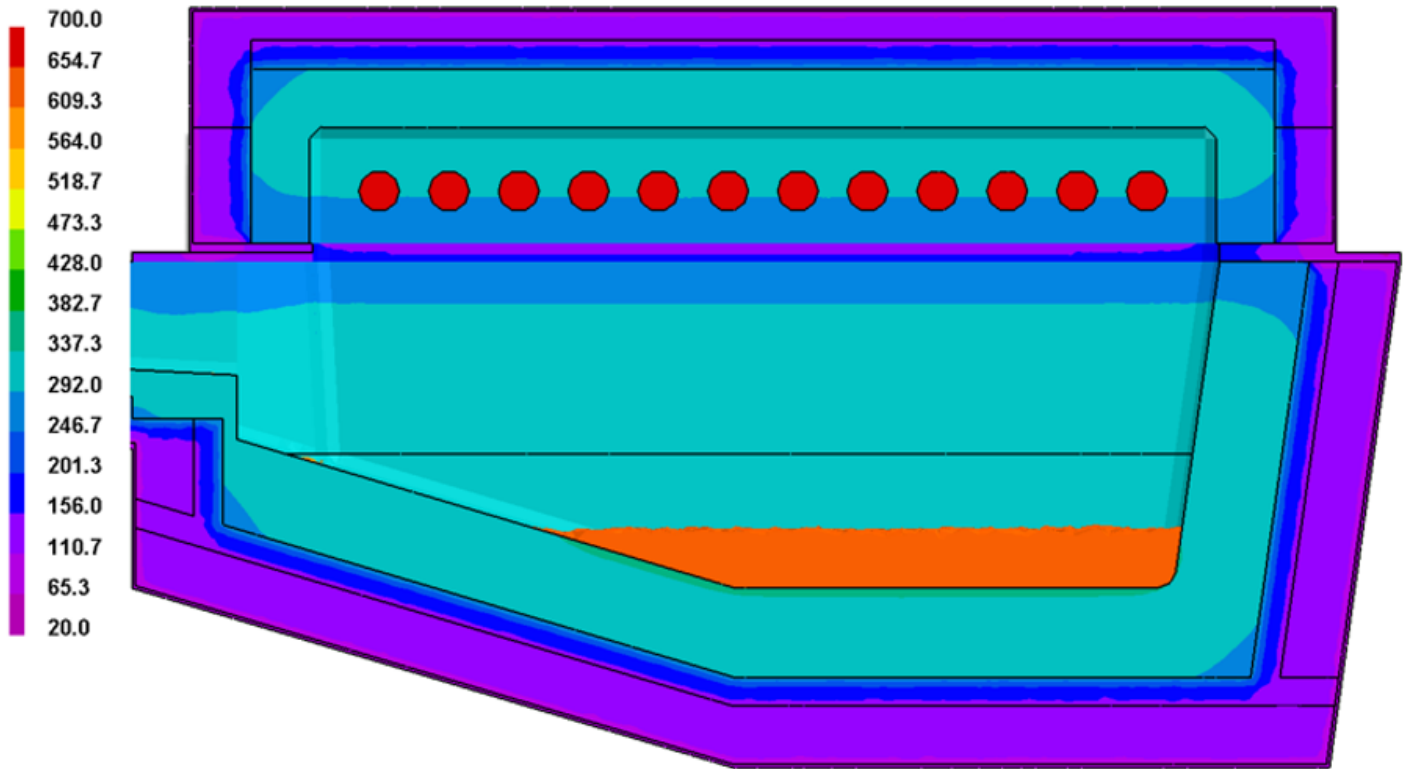


Figure 9

Model of the temperature distribution in the mixer furnace after the melt enters it from the metal track

T, °C

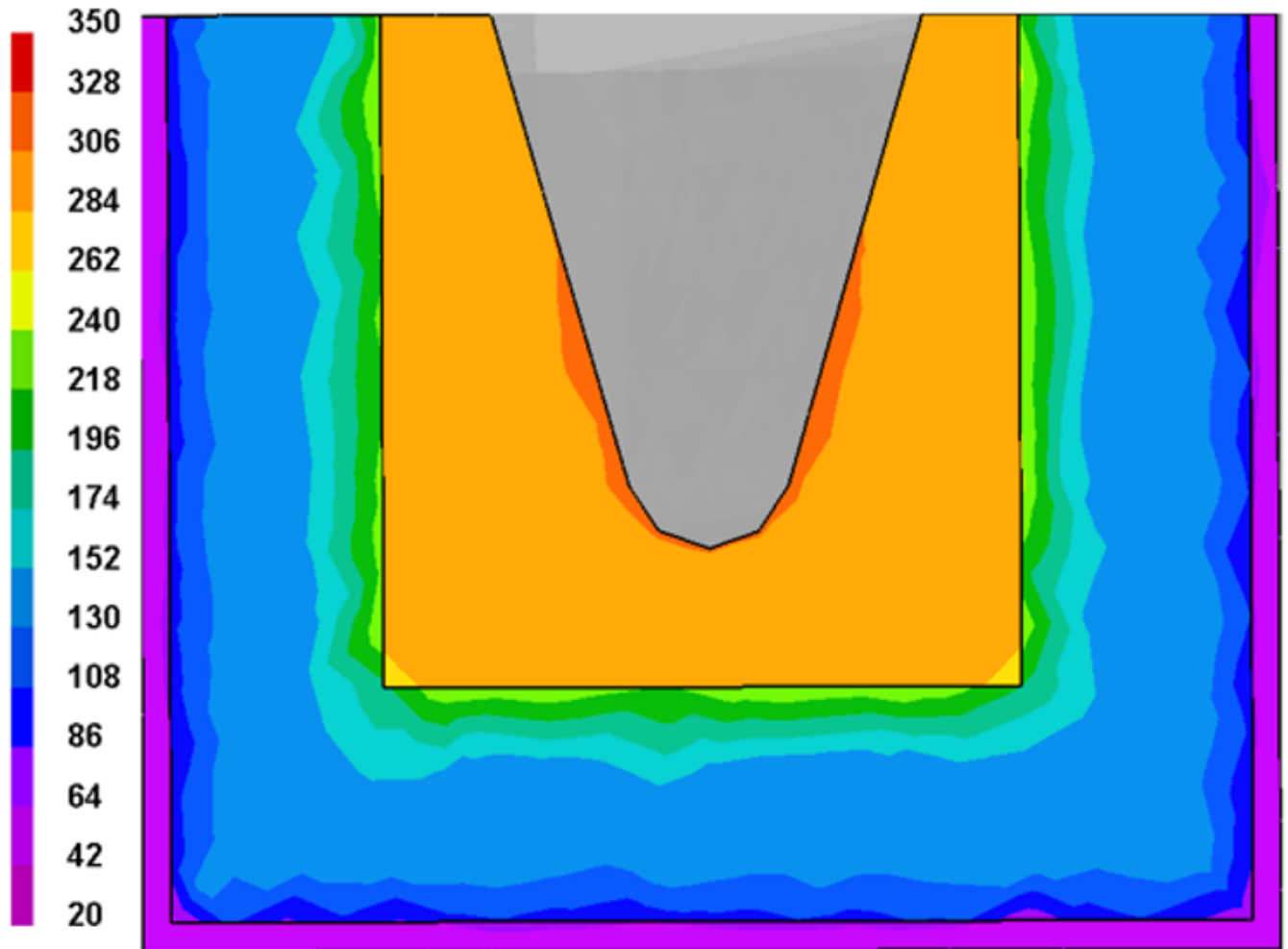
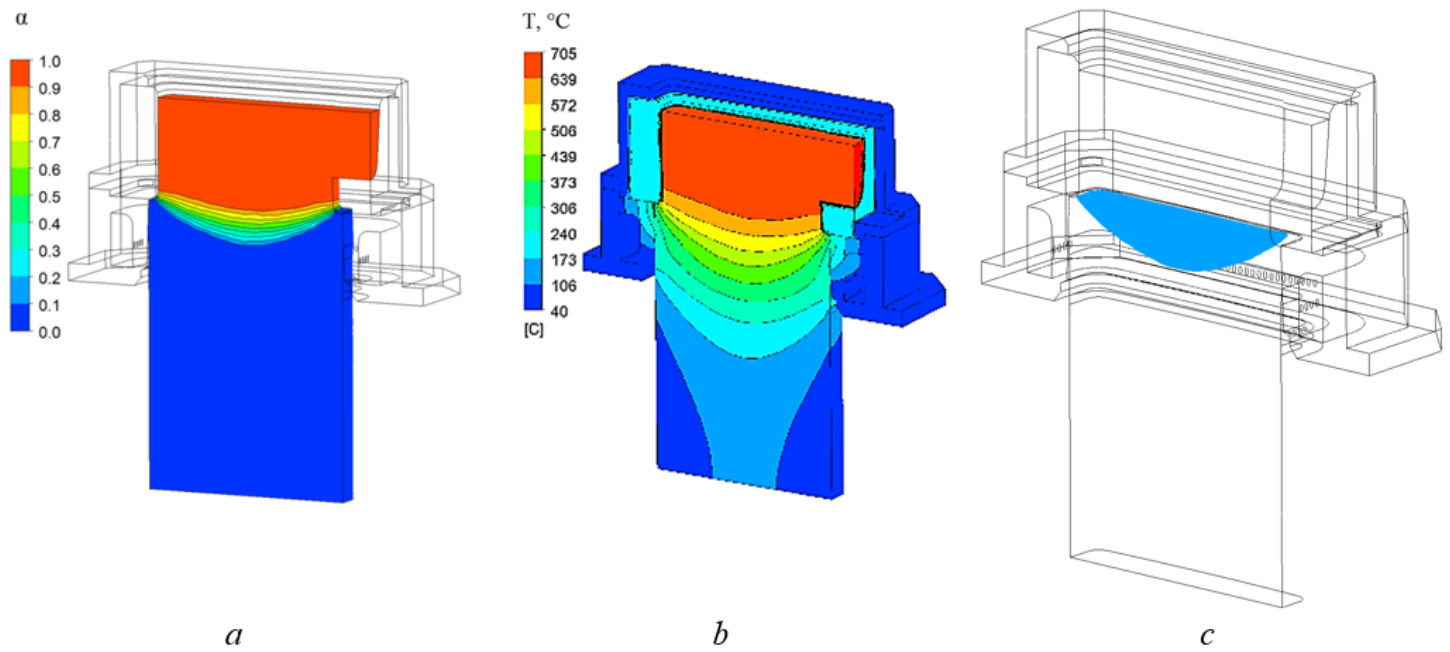


Figure 10

Model of temperature distribution in the cross-section of metal track trays



**Figure 11**

Model of the distribution of the solid phase (a), temperatures over the cross-section of the mold (b) and the profile of the hole (c) according to option 1

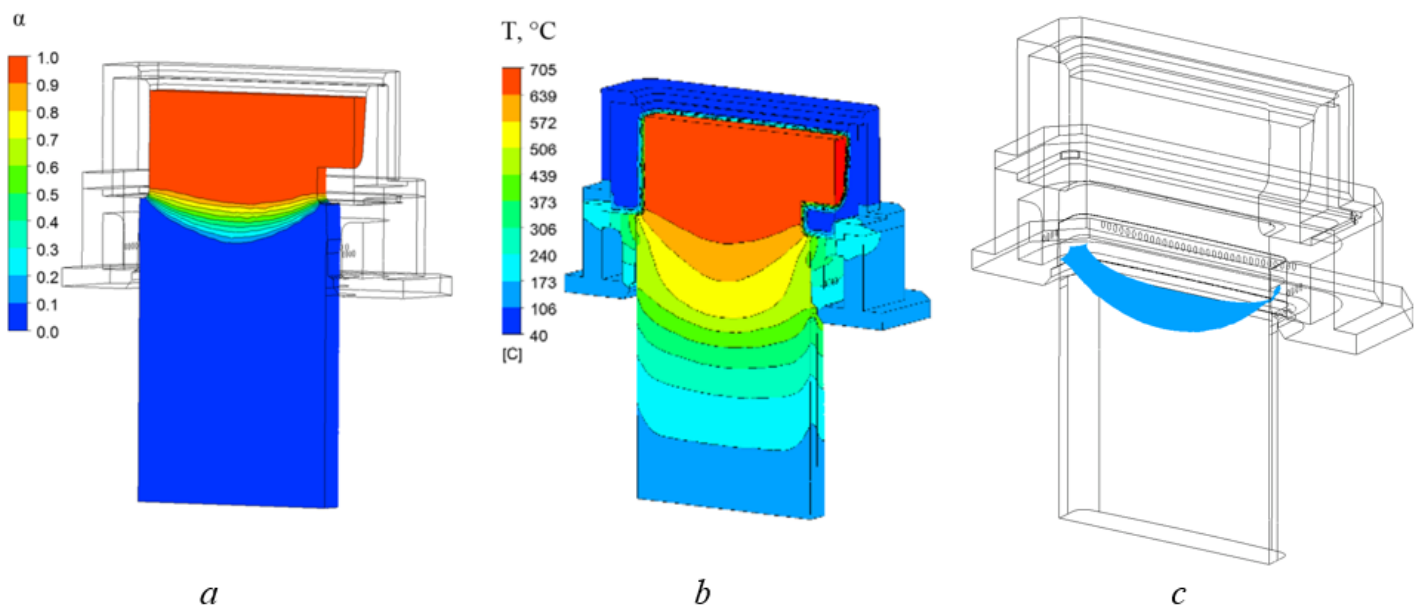


**Figure 12**

Model of the distribution of the solid phase (a), temperatures over the cross-section of the mold (b) and the profile of the hole (c) according to option 2

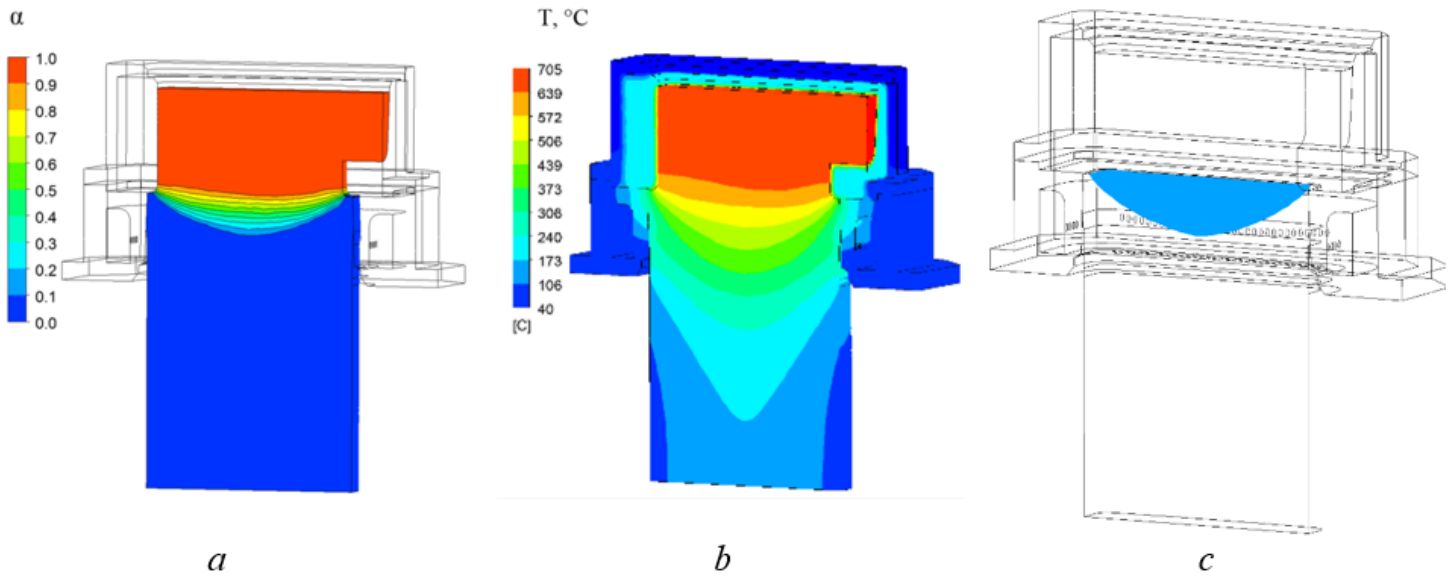


**Figure 13**

Model of the distribution of the solid phase (a), temperatures over the cross-section of the mold (b) and the profile of the hole (c) according to option 3

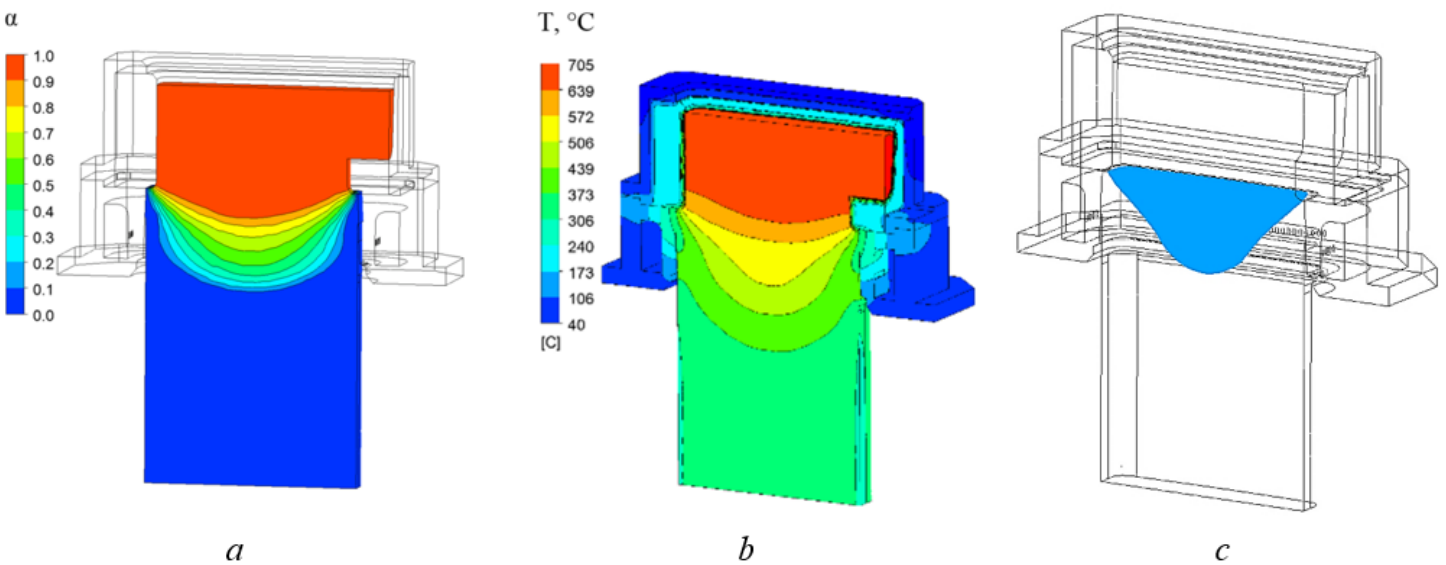


**Figure 14**

Model of the distribution of the solid phase (a), temperatures over the cross-section of the mold (b) and the profile of the hole (c) according to option 4

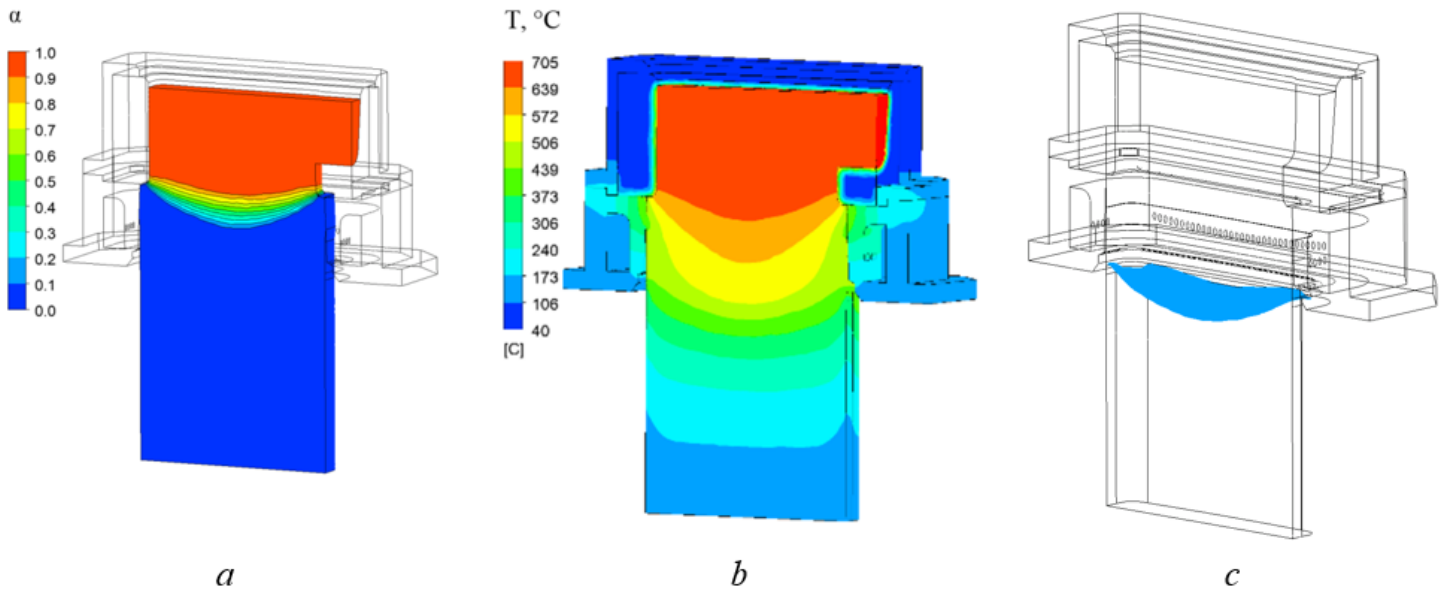


**Figure 15**

Model of the distribution of the solid phase (a), temperatures over the cross-section of the mold (b) and the profile of the hole (c) according to option 5

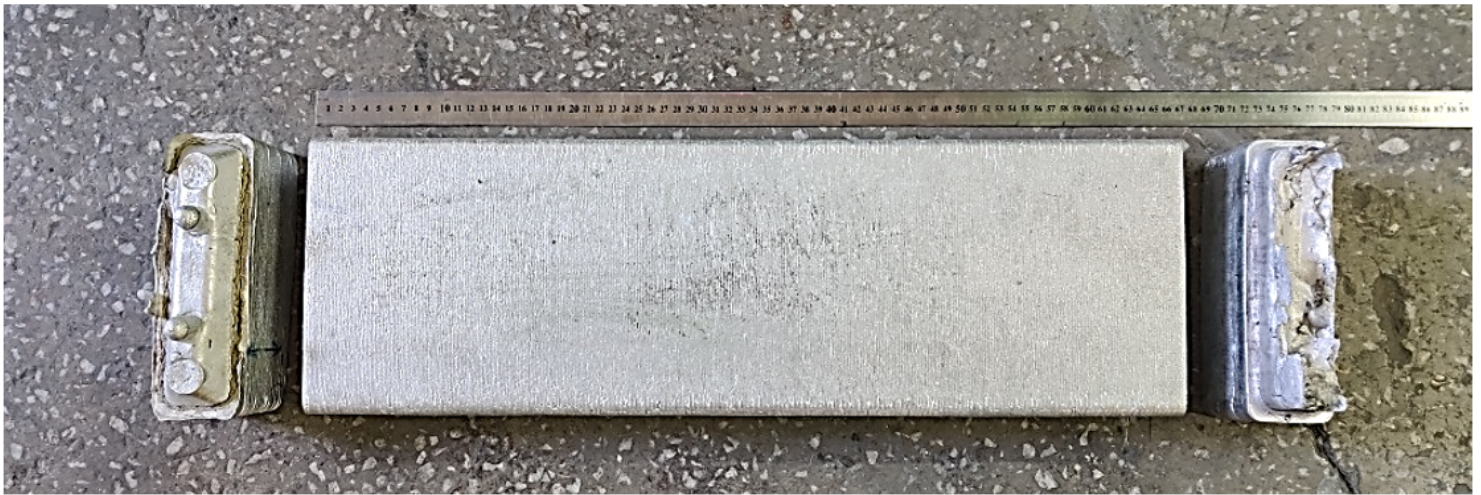


**Figure 16**

Ingot obtained at the SCCU: on the left – bottom part, on the right – gating (top) part

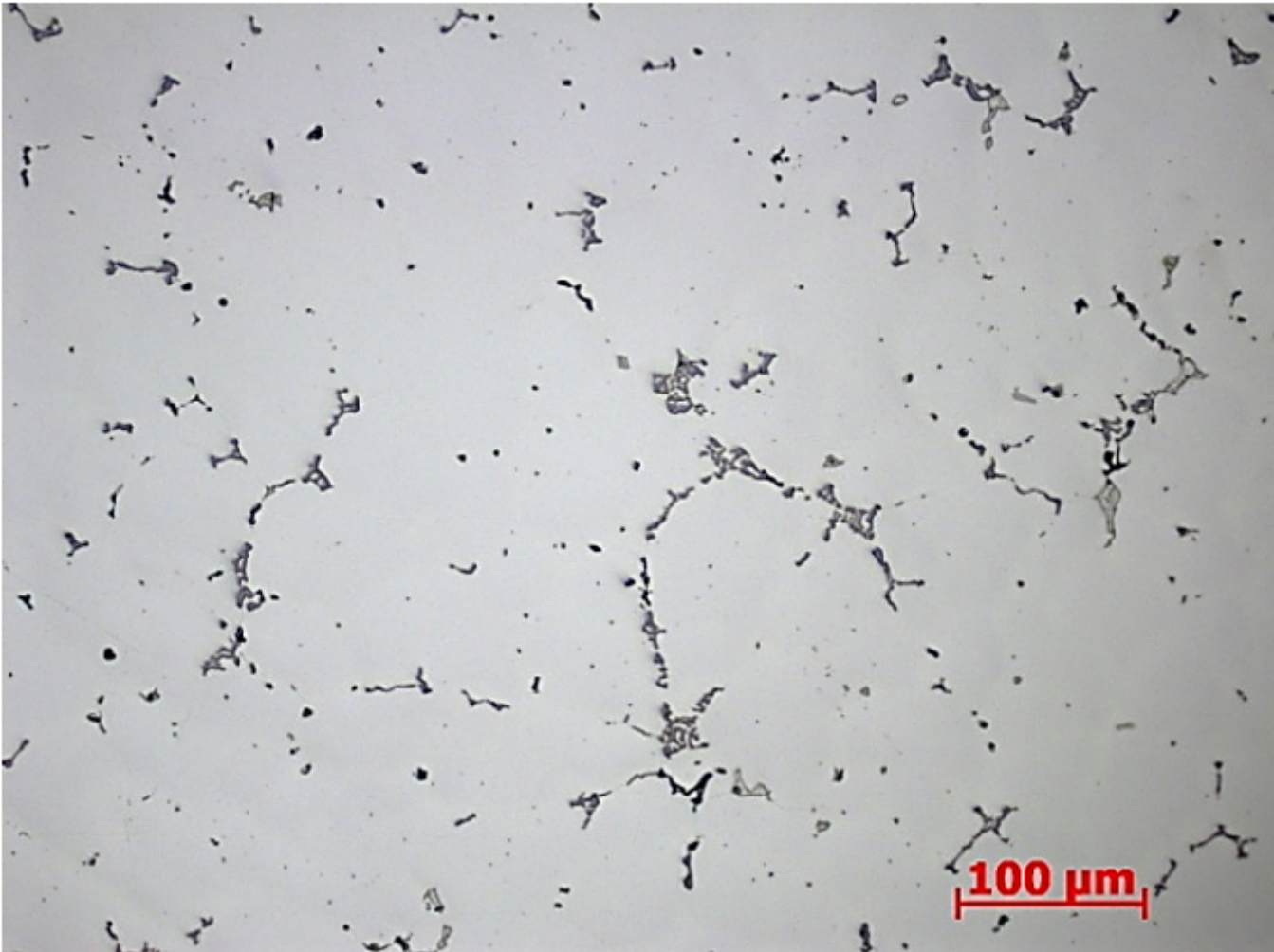
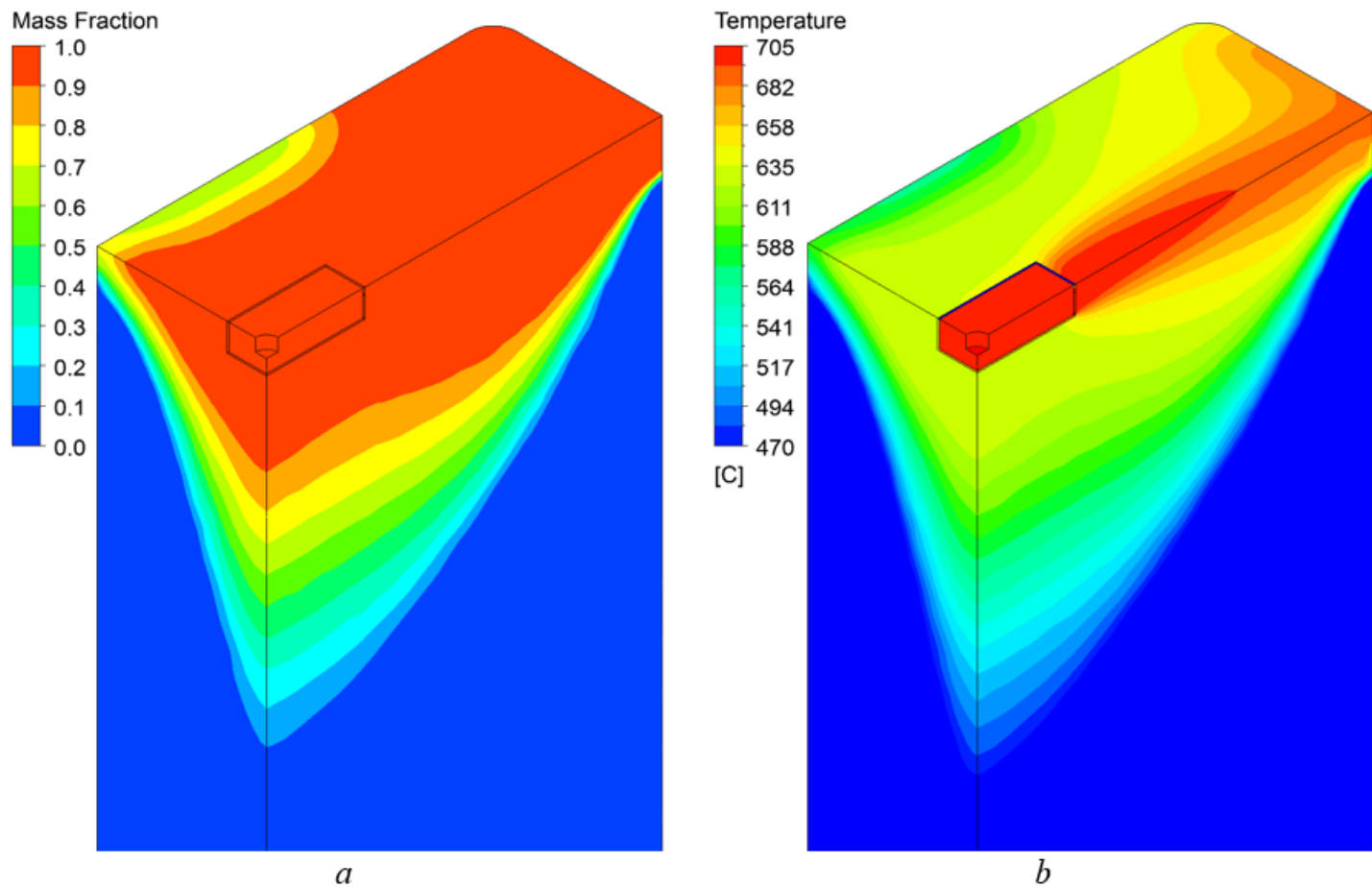


Figure 17

Microstructure of an ingot obtained at the SCCU



**Figure 18**

Model of the distribution of the solid phase (a) and temperature (b) over the section of the mold according to option 5 for the stationary mode of casting an ingot with a section of 1310×560 mm



**Figure 19**

Large-sized ingot with a cross-section of 1310×560 mm, casted in industrial conditions according to the modes obtained by complex modeling, with cut-off bottom and pour parts